Fluctuation analysis of high frequency electric power load in the Czech Republic[☆]

Jiří Kracík

Charles University in Prague, Faculty of Social Sciences, Institute of Economic Studies, Opletalova 26. CZ-11000 Prague 1, Czech Republic

Hynek Lavička[1]

Czech Technical University in Prague, Faculty of Nuclear Sciences and Physical Engineering, Department of Physics, Břehová 7, CZ-11519 Prague 1, Czech Republic

Bogolyubov Laboratory of Theoretical Physics, Joint Institute of Nuclear Research, RU-141980 Dubna, Russia

Abstract

We analyze the electric power load in the Czech Republic (CR) which exhibits a seasonality as well as other oscillations typical for European countries. Moreover, we detect 1/f noise property of electrical power load with extra additional peaks that allows to separate it into a deterministic and stochastic part. We then focus on the analysis of the stochastic part using improved Multi-fractal Detrended Fluctuation Analysis method (MFDFA) to investigate power load datasets with a minute resolution. Extracting the noise part of the signal by using Fourier transform allows us to apply this method to obtain the fluctuation function and to estimate the generalized Hurst exponent together with the correlated Hurst exponent, its improvement for the non-Gaussian datasets. The results exhibit a strong presence of persistent behaviour and the dataset is characterized by a non-Gaussian skewed distribution. There are also indications for the presence of the probability distribution that has heavier tail than the Gaussian distribution.

Keywords: MFDFA, electric power load, Hurst exponent, persistent process, 1/f noise, non-Gaussian distribution

1. Introduction

The responsibility for the safe and reliable operation is one of the basic duties of the national Transmission System Operator (TSO). The gradual liberalization of the European electricity market led to a necessity of the integration of mutually uncoordinated transmission systems. The enhancements of these transmission systems are very intensive in terms of both the time as well as capital investments and due to this the current energy networks are reaching their technical limits. That is mostly obvious in case of a massive increase of the offshore wind power plant installations located in the distant parts, hundreds of kilometers far from the end consumer. The electricity, which cannot pass through the under-dimensioned transmission lines or so called congestions, flows through the surrounding system which must accommodate these unscheduled flows. Unfortunately, the market with electricity and its mechanisms do not reflect this fact. In our work, we analyze high frequency data of electricity consumption in the Czech Republic and we also determine the degree of the uncertainty of the behavior of the consumers.

The analysis of the electricity prices and loads has been discussed by R. Weron [1]. He stated that the electricity loads, which are non-stationary time series, are combinations of both the trends and the periodic cycles with a random component. It is known from literature that electricity loads are correlated with the weather (e.g., the temperature, see [1, 2, 3]) as well as with socio-economical changes and processes.

The first method (R/S method) for a non-stationary time series analysis was invented by H.E. Hurst [4]. Since its introduction the method has been tested on various datasets and also implemented very effectively on computer [5, 6, 7, 8]. The method estimates the Hurst exponent of dataset that is related to the exponent of the autocorrelation function from the theory of fractional Brownian motion [9, 10]. A modern alternative of the Hurst exponent estimation for series with local trends is the Detrended Fluctuation Analysis (DFA) which was introduced in [11, 12] and used for economy datasets [13], heart rate dynamics [14, 15], DNA sequences [16, 12, 11], long-time weather records [17], electricity prices time series [6, 7] and wind speed records [18]. Recently, the DFA was improved to quantify the fluctuation function of datasets using different metrics [19, 20]. The MFDFA is able to estimate the exponent of the autocorrelation function and also the exponent of the probability distribution function. In recent years, there has been a considerable focus on the investigation of multifractal cross-correlation between a pair of synchronized datasets [21].

There is a broad literature of modelling and forecasting methods of both price and/or load time series. It usually incorportes the Autoregressive Moving Average processes (ARMA), the Vector Autoregression (VAR), the Vector Error Correction (VECM), machine learning, an adaptive neuro-fuzzy network and a customers segmentation. Fixed mean, restricted variance and normally distributed error term represent basic assumptions for finding the best linear unbiased estimation, for a summary see Ref [22, 23, 24].

In this paper we study a dataset of electric power load in the Czech Republic
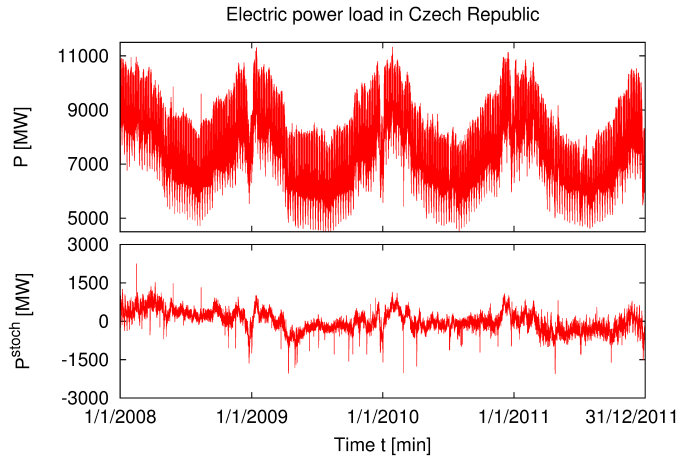
Figure 1: The electric power load in Czech Republic between January 1st 2008 and December 31st 2011 (top) and the stochastic part P^{stoch} obtained by the filtration of the signal (bottom).

since 2008 till 2011 with a one-minute time step. We focus on the properties of the fluctuation function where the first periodic part of the signal is filtered from the dataset and then the MFDFA is used. Our main aim is to determine the Hurst exponent which provides information about the autocorrelation function as well as the probability distribution. We also validate the assumptions of the normal (Gaussian) noise distribution and the short-range correlations.

The paper is organized as follows: In section 2 we describe the methodology of data processing. We first describe the Fourier filtering method and then the MFDFA. In section 3 we analyze the dataset using the methodology from section 2. Finally, in section 4, we draw the conclusions of our study.

2. Methodology

Human behavior datasets typically exhibit the oscillations with the periods related to the units of calendar [1, 17] and the same applies to the electric power load. The one-year and one-week oscillations are clearly visible in Fig. 1 but the presence of other frequencies is not so easily observable. To obtain the information regarding the strength of the oscillations we employ the Power spectrum which is shown in Fig. 2. It depicts additional periods with the lengths of one day and 12 hours beside the others. Moreover, since the periods of the power loads do not follow harmonic functions, we can also observe peaks at the positions of the integer multiples of a typical trend. The reconstruction of the original load on the basis of these most significant trend components is influenced by randomness which is represented by less significant components of the Power spectrum.
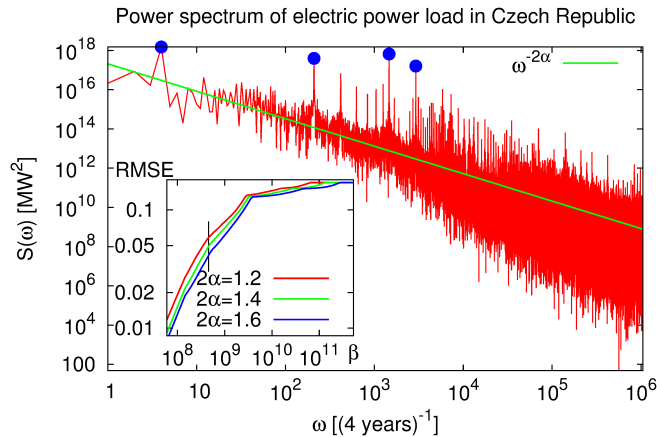
3

Figure 2: The power spectrum of the electric power load between 1st of January 2008 and 31st of December 2011 spanning 4 years in total showing the 1/f property with the extra peaks. The blue points show one-year (Y), one-week (W), one-day (D) and 12 hour periods (12H). In the inset of the plot, there is the dependence of the RMSE on β for the different exponents of filtration (parameter α). The vertical black line shows the actual location of the parameter β used for the filtration procedure.

2.1. Motivation

In our study, we focus on the properties of the random part and we use the MFDFA which is popular among scientists [6, 11, 12, 14, 15, 13, 19, 20, 25] as an effective tool for extracting the properties of a long-range memory within the time series.

Since time series generally might be non-stationary, polynomial trends may still govern them. The basic idea of the DFA is to strip off the trends and use the residues for the further analysis. In the MFDFA, we are looking for typical patterns, which govern the time series manifesting a self-affine property defined by $X(c \cdot t) = c^H \cdot X(t)$. The generalized Hurst exponent H, determined by the method, is the measure of the long term memory in the time series and it is directly related to the non-integer fractal dimension D.

The disadvantage of this method is that the periodic trends disturb the estimation of the Hurst exponent [26] and therefore, before we employ the method, we have to filter out the oscillations from the signal.

We use the Fourier transform to execute the filtration. The MFDFA itself then removes the polynomial trends. The resulting signal is decomposed as

$$P(t) = P^{stoch}(t) + P^{deter}(t), \tag{1}$$

where P^{deter} describes the periodic behavior of the system, while P^{stoch} stands for the random part.

We used a regression model with dummy variables indicating holidays and we perform the method described below. We observed negligible differencies for the low orders of the MFDFA but the observable differences for the higher orders of the MFDFA. However, the widths of the multifractal spectrums are negligible in both cases.

2.2. Mathematical description

We execute our analysis in three steps. First, we perform the Fourier transform to separate the signal into the stochastic and the deterministic part by the Fourier transform. In the next step, we execute the MFDFA. Finally, in the last step, we calculate the correlated Hurst exponent, which requires shuffling of the original-time series. It is an improvement of the typically used generalized Hurst exponent, exploited in cases, where we have an assumption of the non-normally distributed time series.

2.2.1. Fourier transform filtering

We deal with a signal in the discrete time-steps $P(t_n)$ where $t_n = t_1 + n \cdot \Delta t$ and $n \in M \equiv \{1, \ldots, N\}$. Since the Discrete Fourier Transform of the signal is $\widehat{P}(m) = \frac{1}{\sqrt{N}} \sum_{n \in M} \exp\left(-\frac{2\pi i \cdot n \cdot m}{M}\right) P(t_n)$, and the related Power spectrum $S(m) = \widehat{P}(m) \cdot \widehat{P}^*(m)$, where x^* stands for conjugation). The Power spectrum, see Fig. 2, of the signal $P(t_n)$ exhibits a power law-like shape with extra peaks and each coefficient of the Fourier transform is separated into two parts according to the threshold $\beta \cdot m^{-\alpha}$:

- discrete significant coefficients in the Power spectrum for certain frequencies above the threshold forms $|\widehat{P^{deter}}(m)|$;

- coefficients below the threshold forms $\widehat{P^{stoch}}(m)$;

where α and β are the parameters set with regard to the chosen RMSE level. We also note that if $\widehat{P^{deter}}(m) \neq 0$ then we define $\arg \widehat{P^{deter}}(m) = \arg \widehat{P^{stoch}}(m) = \arg \widehat{P}(m)$. Otherwise $\arg \widehat{P^{deter}}(m)$ is not defined. The Fourier transform of the sub-signals $\widehat{P^{deter}}(m)$ and $\widehat{P^{stoch}}(m)$ then follow $\widehat{P}(m) = \widehat{P^{deter}}(m) + \widehat{P^{stoch}}(m)$, which is the Fourier transform of Eq. 1. By executing the the inverse Fourier transform $P(t_n) = \frac{1}{\sqrt{N}} \sum_{n \in M} \exp\left(\frac{2\pi i \cdot n \cdot m}{M}\right) \widehat{P}(m)$ we obtain a deterministic part $P^{deter}(t_n)$ from $\widehat{P^{deter}}(m)$. The later part $\widehat{P^{stoch}}(m)$ is transformed to $P^{stoch}(t)$.

To measure the quality of the filter we use a root mean square error, see inset of Fig. 2, defined as follows:

$$RMSE = \frac{\sqrt{N \sum_{i=1}^{N} \left(P^{deter}(t_i) - P(t_i)\right)^2}}{\sum_{i=1}^{N} P(t_i)}. \qquad (2)$$

The level of the error was determined both to decrease the RMSE and to prevent P^{stoch} from incorporating a periodic function that produces the artificial behavior of the fluctuation function.

2.2.2. Multi-fractal Detrended Fluctuation Analysis

We employ the Multi-fractal Detrended Fluctuation Analysis (MFDFA) for analyzing the filtered signal $P^{stoch}(t_i)$. The method is employed as an effective tool to avoid the artificial behaviour (see Ref. [27]) in the autocorrelation function or in the Power spectrum due to the oscillation of the electric power loads and the presence of the peaks in the Power spectrum, see Fig. 2.

Each element $\{x_i \equiv P^{stoch}(t_i)\}$ of the dataset is indexed by $i \in M$. The application of the MFDFA consists of five steps:

Step 1. Integration of the dataset to produce the dataset $X_j = \sum_{i=1}^{j} x_i$. The "double" integration of the dataset $\tilde{X}_j = \sum_{i=1}^{j} X_i$ is also performed.

Step 2. Division of the dataset X_i into $L_s \equiv \lfloor \frac{N}{t} \rfloor$ overlapping segments $X_{j,k}$ with length s and $j \in \{1, \ldots, s\}$.

Step 3. Use of a standard (least-square) regression method of fixed order M on each segment $X_{j,k}$ to obtain the local trend $T_k(x)$ in the region $x \in [1, s]$.

Step 4. Calculation of the sample variance for each of the L_s segments of the original dataset

$$V(k) \equiv \frac{1}{s} \sum_{j=1}^{s} (X_{j,k} - T_k(j))^2 . \tag{3}$$

Step 5. Averaging over all the segments of the original dataset to obtain the multi-fractal fluctuation function

$$F_q(s) \equiv \begin{cases} \left(\frac{1}{L_s} \sum_{k=1}^{L_s} V^{\frac{q}{2}}(k) \right)^{\frac{1}{q}} & \text{if } q \neq 0 \\ \exp\left(\frac{1}{2 \cdot L_s} \sum_{k=1}^{L_s} \ln V(k) \right) & \text{if } q = 0 \end{cases} . \tag{4}$$

In the analysis we investigate the properties of the fluctuation function $F_q(s)$ on the window of the size s and on the measure q. Generally, $F_q(s)$ grows with increasing s for all q (see Fig. 4 or follow original literature [19, 20, 26, 12, 11, 14, 28]), following the power law

$$F_q(s) \quad \sim \quad s^{H(q)+1}. \tag{5}$$

The exponent $H(q)$ is called the Hurst exponent, see Ref. [4]. Generally, it is related to the long-term autocorrelation or the heavy-tailed distribution of the governing process, see Ref. [19, 20]. We also note that $+1$ in Eq. 5 stands due to the application of the double integration instead of the single integration of dataset, for discussion, please, see Ref. [19].

We exploit a fractal spectrum to analyze whether the dataset is governed by a single exponent or by a set of exponents. We define a scaling function by formula:

$$\tau(q) = q \cdot H(q) - 1. \tag{6}$$

We define a fractal spectrum as the Legendre transform of $\tau(q)$ using the definition of a new variable $\pi = \frac{d\tau}{dq}$:

6

$$f\left(\pi\right) = q \cdot \pi - \tau. \tag{7}$$

Generally, the fractal spectrum allows to distinguish mono- and multifractal processes. The width of the fractal spectrum is defined by the formula $\Delta\pi = \max_{q\in\mathbb{R}} \pi - \min_{q\in\mathbb{R}} \pi$. The value of π in peak of $f\left(\pi\right)$ denoted by π^{max} represents the most frequent value of the exponent. As the width of the fractal spectrum goes wider, the number of admitted exponents increases and the monofractality shifts to the multifractality.

2.2.3. Shuffling of the stochastic part of the time series

Generally, if a stochastic process generates the time series following a non-normal (non-Gaussian) distribution, the generalized Hurst exponent $H\left(q\right)$ combines the information about the autocorrelation function influenced by the properties of its probability distribution. We extract the correlation Hurst exponent $H^{cor}\left(q\right)$ that separates the generalized Hurst exponents calculated using the original time series and calculated using the shuffled one[1].

While executing the shuffling procedure, we destroy the autocorrelations (if present) within the sample. Then we use a standard MFDFA described in previous section to the calculate shuffled fluctuation function:

$$F_q^{shuf}(s) = \overline{F_q\left(\{x_i\}^{shuf}\right)(s)},$$

where $\overline{x}$ stands for the averaging samples of shuffling and $\{x_i\}^{shuf}$ means shuffling of the time serie x_i. Finally, we estimate the generalized Hurst exponent of the shuffled time serie $H^{shuf}\left(q\right)$. As it was noted in the previous paragraph, the correlation Hurst exponent is then defined by following formula:

$$H^{cor}(q) = H(q) - H^{shuf}(q). \tag{8}$$

Analogically to the generalized Hurst exponent $H\left(q\right)$ we can define the correlation fractal spectrum $f^{cor}\left(\alpha\right)$ related to $H^{cor}\left(q\right)$ by the formulas 6 and 7.

2.3. Implementation of the method

We used a multi-threaded implementation of the MFDFA with Zarja library [29] [2] which can effectively run on multi-core cluster computers. We also compared the results with the implementations used in [28, 16, 14]. The filtration of dataset was executed in the Python using the NumPy and SciPy modules [30, 31].
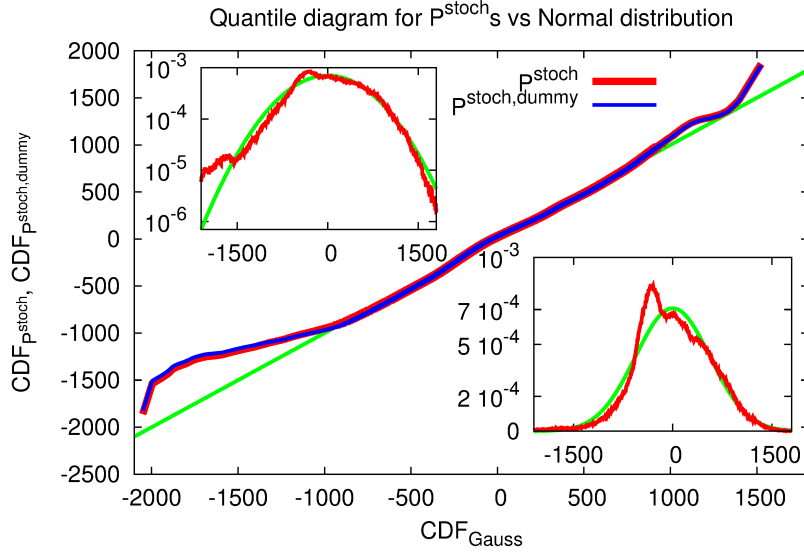
Figure 3: The quantile diagram of the probability density function generated from P^{stoch} and its counterpart generated from it by the regression model with dummy variables $P^{stoch,dummy}$ and their comparison with the normal distribution with the same mean μ and variance σ^2. In the insets, we show the comparison of the probability density functions of P^{stoch} with the appropriate normal distribution (the normal plot at the bottom, the log-normal scale at the top).

3. Analysis of dataset

3.1. Data description

Our dataset describes the electric power load of the Czech Republic which is monitored by national Transmission System Operator (TSO), ČEPS a.s. It was calculated with high frequency from the stored data using the formula:

$$P(t) = \sum_{i \in 1}^{M} T(t,i) - E(t) + I(t) + P_u(t), \qquad (9)$$

where $T(t,i)$ stands for i-th turbo-generator output of the total number M. The turbo-generators are directly measured from their minimal value of 100 kW of installed capacity. $E(t)$ and $I(t)$ are the exports and imports, respectively. Generally, they are a kind of bottlenecks because there are only few direct

---

[1]To shuffle the dataset we utilized Fisher-Yates algorithm that is effective even in the case of large dataset. In our case, we used the average of 100 samples of shuffling.
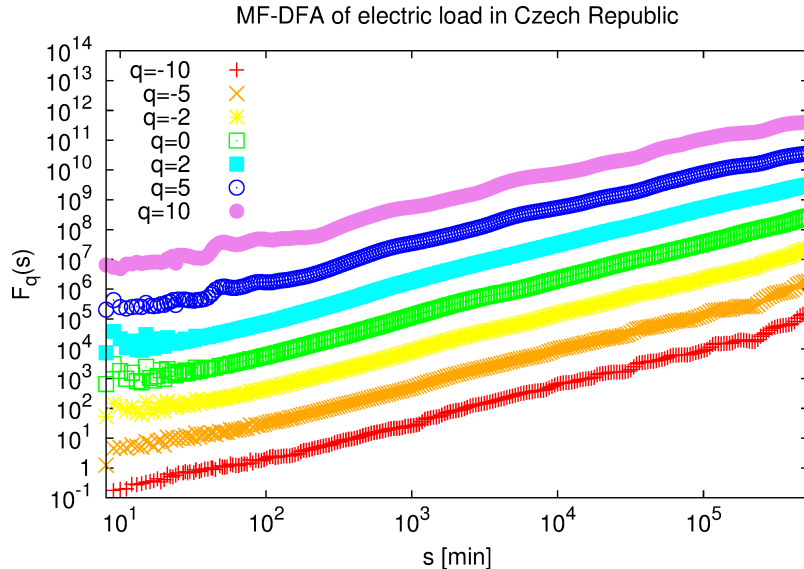
[2]Source code can be found at http://zarja.sourceforge.net.

Figure 4: The fluctuation function $F_q(s)$ of the signal P^{stoch} obtained using the MFDFA of the order 4 for various qs. We present $q \in \{-10, -5, -2, 0, 2, 5, 10\}$ from the bottom to the top, respectively. Each plot is multiplied by factor 10 from its predecessor.

transmission lines between the Czech Republic and the neighboring countries. Finally, $P_u(t)$ stands for the balance of the pumped-storage hydroelectricity[3].

The dataset is calculated in real time from various sources and the datalinks are not generally completely error-proof. Each datapoint is thus accompanied with the confidence flag indicating the credibility of the source. Some datapoints are calculated, using Eq. 9, others are interpolated.

Our dataset consists of $N = 2,103,840$ datapoints and it spans 4 years since 2008 till 2011 with a one-minute time step. In our analysis, we neglect the confidence flag and we use the electric power load measured in MW only.

3.2. Results of Fourier filtering

The electric power load dataset of the Czech Republic is depicted in Fig. 1, where the Power spectrum $S(\omega)$ exhibits the power law with extra significant peaks, see Fig. 2, and therefore we first execute the Fourier filtering of the dataset where we assume $|\widehat{P^{stoch}}(m)| = \beta \cdot m^{-\alpha}$ with parameters α and β yet to be determined. In our study we mainly choose $\alpha = 0.7$ as an approximation of the best fit of this exponent and in order to the prove robustness of the method, we also plot the $RMSE$ for the two other values close to the chosen value of

---

[3]There are three of them - Dlouhé stráně 600 MW, Dalešice 450 MW and Štěchovice with 48 MW of installed capacity.
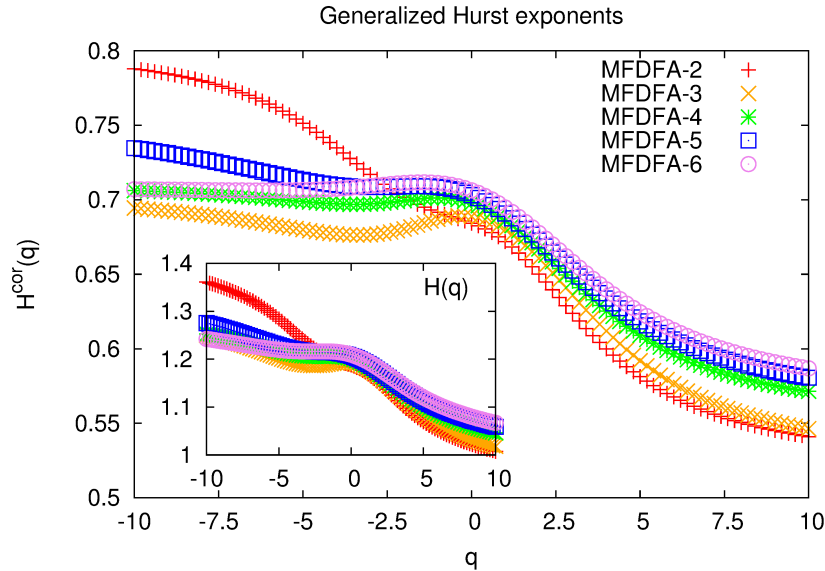
Figure 5: The correlation Hurst exponent $H^{cor}(q)$ estimated using the MFDFA of orders $2-6$. In the inset, we show the generalized Hurst exponent $H(q)$ for the same MFDFA orders. We used the dataset obtained by the regression model with dummy variables indicating the holidays. The dataset without use of the method follows the analogous pattern.

the parameter α, see inset of Fig. 2. The extensive test of the dependence of the fractal spectra on the exponent α is shown in Fig. 6.

Then we construct the dependence of the $RMSE$ on the parameter α and we choose the break-point of this dependence as an α value. The $RMSE$ is defined by Eq. 2 and at $\beta = 7 \cdot 10^8$ MW (we note that it is the equivalent of $S(m) \sim m^{-2\alpha}$). The P^{stoch} does not exhibit large periodic fluctuations (see the bottom part of Fig. 1) and the quantile diagram as well as the probability density distribution around the mean behave close to the normal (Gaussian) distribution (Fig. 3). We note that the choice of $\beta = 2 \cdot 10^9$ MW leads to both the significant deviation from normal distribution in its center part as well as to the increase of the periodicity in the stochastic part. The filtered signal is shown at the bottom of Fig. 1 and it is then more analyzed.

3.3. Results of application of MFDFA

Firstly, we investigate the probability distribution function of the time series P^{stoch} despite of the fact that there can still be temporary trends, see Fig. 3. The comparison of the quantile diagram, the mean and the variance of P^{stoch} with quantiles of the normal (Gaussian) distribution is presented in Fig. 3. It clearly shows the deviations for the small values of the power load. In the lower right inset in Fig. 3, the comparison of the histogram of P^{stoch} with the appropriate normal distribution exhibits a good approximation about the
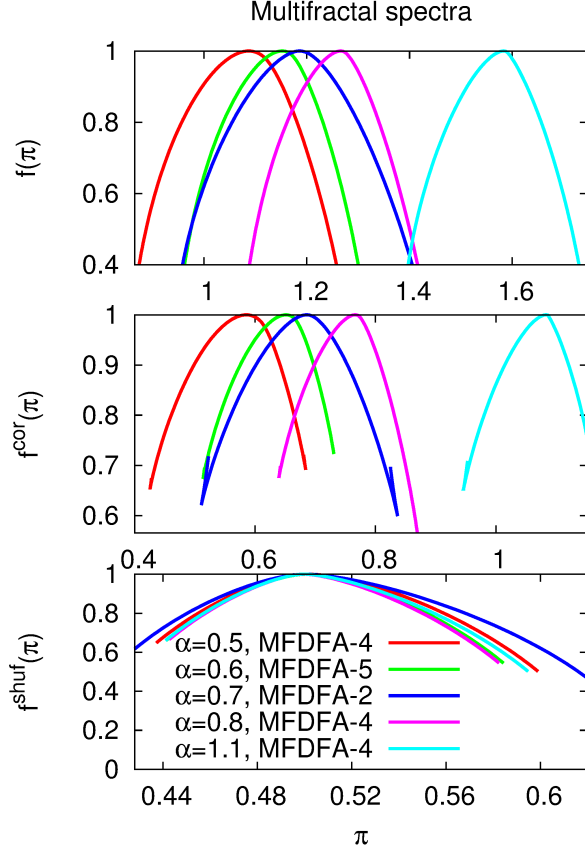
Figure 6: The multifractal spectrum $f(\pi)$ of P^{stoch} for various orders of the MFDFA method and initial detreding with parameter α is shown on the top. In the middle we present the correlation and shuffled multifractal spectrum, respectively.

average. In the upper left inset in Fig. 3, we can observe the deviations of the small values of the power load from the normal distribution in the semi-logarithmic scale.

In the next step, we perform the MFDFA to calculate the fluctuation function $F_q(s)$ and we estimate the generalized Hurst exponent $H(q)$, see the inset of Fig. 5 in range $[2 \cdot 10^3, 2 \cdot 10^5]$. The generalized Hurst exponent depends on q we expect presence of multifractality. To get valuable information about the autocorrelation function, we shuffle the dataset to calculate the fluctuation function $F_q^{shuf}(s)$. The ratio of the original fluctuation function $F_q(s)$ against the fluctuation function of the shuffled dataset $F_q^{shuf}(s)$ formulated as $F_q^{cor}(s) = \frac{F_q(s)}{F_q^{shuf}(s)}$ follows the power law similarily as $F_q(s)$ see Fig. 4. Then the calculation of the correlation Hurst exponent $H_q^{cor}(s)$ is performed using the formula 8. We show $H_q^{cor}(s)$ in Fig. 5 and the exponent stands between
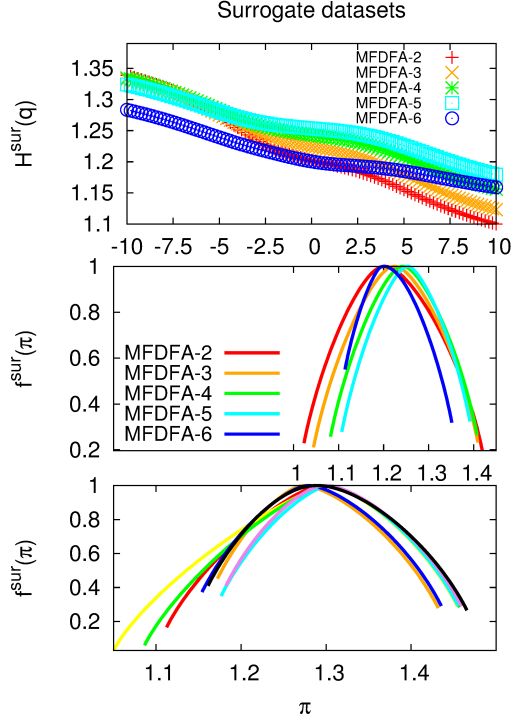
Figure 7: The generalized Hurst exponents (top) and the multifractal spectrums (middle, bottom) of the surrogate datasets which underwent phase randomization. The middle figure show the multifractal spectrums for the surogate dataset and bottom one illustrates dependence on the subset of the dataset (each color shows the different subset). The top and middle figure plots dependence on the order of the method. The bottom subplot is for order 4 of the method.

the values of 0.55 till 0.8 (in contradiction to the calculation of the generalized Hurst exponent based on the normally distributed time series), showing a strong persistence. Additionally we note that the estimation of the Hurst exponents is stable with regard to the orders of the MFDFA.

In Fig. 6, the fractal spectrum $f(\pi)$, the correlation fractal spectrum $f^{cor}(\pi)$ and also the shuffled fractal spectrum $f^{shuf}(\pi)$ of the stochastic part P^{stoch} are not concentrated at single π but they are broadly spread among the wide range of πs. conclude that the processes are multifractal in the distribution as well as in the correlation function. However, multifractality of the correlation function is stronger $\Delta\pi^{cor} \cong 0.3$ in contrast to the multifractality of the distribution function $\Delta\pi^{shuf} = 0.15$ for the same order of the method.

3.4. Tests of stability of the results

The above mentioned results of the analysis may depend on additional factors. To address the factors we execute additional tests to show the invariance of the conclusions.

3.4.1. Stability of results with respect to the filter

As a test of the stability of the results, we performed multiple calculations of MFDFA for different values of the parameters α and β. The generalized Hurst exponent as well as the fractal spectrum depend on a particular value of α and it is independent on the order of the method, see Fig. 6. The change of the order does not significantly imply the change of the width of the fractal spectra. On the other hand, the shuffled fractal spectrum is independent on the value of α and it is localized around $\frac{1}{2}$ – the value of the Gaussian distribution. The persistence of the time series is conserved in the proximity of $\alpha = 0.7$, see the middle of the Fig. 6.

3.4.2. Surrogate data test

Generally, there are usually two reasons of the multifractality in time series:

- long range correlations of small and large fluctuations within the time serie;

- heavy-tailed probability distribution function (not necessarily the Lévy α-stable distribution, see Ref. [32]).

The long-range correlation property and the fat-tailed probability distribution are investigated by shuffling and by a phase randomization. Shuffling destroys the correlations within the time series but it preserves the probability distribution. On the other hand, the phase randomization preserves the correlation function but weakens both the non-Gaussian and non-linear properties of the time serie. The procedures were firstly proposed in Ref. [33] and a review of its use can be found in Ref. [34]. We note that this method was initially used in the context of the MFDFA in Ref. [35].

We practically performed the test on 50 samples of the surrogate datasets and we present the results in Fig. 7. In the graph in the top we can see similar results of H as in the inset in the Fig. 5. In the middle graphs there is the result comparable with the top graphs in the Fig. 6. We obtained the width of the fractal spectra $\Delta\pi \cong 0.3$ and the location of the maximum is around $\pi^{max} \cong 1.2$. We conclude that the multifractality is not caused by non-linearity and beside that there are the indications of the presence of a distribution with the tail heavier than the Gaussian distribution possess. From theory of the stable distributions and the stochastic processes, Refs. [32, 36], the Gaussian distribution possess $H(2) = \frac{1}{2}$ and the Lévy α-stable distribution $H(2) = \frac{1}{\omega}$ where ω is the exponent of the tail (for the Gaussian distribution we have $\omega = 2$). We obtained for the shuffled multifractal spectra, where shuffling erases the autocorrelations with in the time series, see the bottom of Fig. 6, wide peak around $\pi^{shuf} = \frac{1}{2}$. Based on the assumption that the probability distribution is stable we admit presence the Lévy α-stable distribution with the exponents ω close to the values of the Gaussian distribution. We also note that the result is independent of the set up of the initial filtering method. Additionally the Lévy α-stable distribution must be skewed due to indications in Fig. . We also tested

the influence of using a regression model with dummy variables for the decrease of the effect of holidays. As you can see on Fig. 3, the result is not significant.

3.4.3. Problems of stationarity and deficient random generators

We applied the Augmented Durbin-Watson test on the P_{stoch} and we rejected the null hypothesis of non-stationarity at the 5% significance level.

As a test of the stability of the results we separated the original dataset into 8 sets with equal size and we executed the proposed method for each segment. The results of the method are at the bottom of Fig. 7 where the curves representing the surrogate fractal spectra show the overlap with the width of fractal spectra $\Delta \pi^{sur} \cong 0.3$ and $\pi^{max} \cong 1.3$. These values are approximately equal to the results of the complete dataset. Thus, we conclude, that the results of the method are stable with the respect to the change of the scale.

4. Conclusions and Outlook

The main contribution of this paper is an analysis of the high-frequency electric power loads dataset of the Czech Republic using the improved MFDFA methodology. We discovered that the power spectrum of the signal exhibits 1/f noise property with the additional peaks that are caused by a periodic behavior of the electricity consumption. Based on that fact, we first separated the noise from modulating signal and then we applied the MFDFA without dealing with an artificial behavior of the fluctuation function, see Ref. [26]. After that we exploited the MFDFA for the analysis of the dataset to obtain information about the autocorrelation function. The major part of the power load is governed by oscillations. Beside that we report a strong persistence of the power loads where the distribution function exhibits non-Gaussian properties. The fractal spectra of both the distribution as well as the autocorrelation function indicate the presence of multifractality. We also performed a test using surrogate datasets as well as a test of stationarity to validate the strength of our conclusions. The analysis suggests the presence of the probability distribution with the tails heavier than the Gaussian distribution.

Some of our results are in contradiction with the previously published work analyzing electricity consumption and also with the assumptions of electricity load prediction models [37, 1, 38, 39]. First, our analysis indicates that the stochastic part of the signal is not normally distributed, second, the distribution function is skewed and it may even have infinite moments of the probability distribution and third, the autocorrelation function is persistent. We also conclude that the estimations of risks based on traditional forecasting methods using the Gaussian distribution and short-range correlations are not usable due to both the long-range autocorrelation and the probability distribution's extremes. The main part of the load constituting approximately 95% of the signal was filtered out and it is systematically driven by external factors. Modeling by means of a regime-switching model makes a good sense to us.

The Czech transmission system is sufficiently dimensioned to cope with electricity consumption fluctuations contained in the dataset we had at our disposal.

The problem that attracts actual attention of the TSO is dealing with the unexpected flows from north to south of Europe through the Czech Republic, see Ref. [40], which are caused by inhomogeneity of sources generating electricity and consumption of electricity in Europe. The presented approach might also be applied to solve a more complex problem, where in addition to the uncertainty of the electricity consumption, we may also consider the uncertainty caused by real power inflows and outflows (imported and exported electricity) or the uncertainty due to differences between cross-border trading and real electricity flows (obeying Kirchhoff's laws). The level of uncertainty is expressed as a deviation from foreseeable behavior described by polynomial trends and periodic oscillations.

Author contributions

J.K. obtained and prepared the dataset. H.L. prepared the tool for analysis and performed the analysis. J.K. and H.L. contributed to the writing of the manuscript. The work described in this paper will be used in J.K.'s Ph.D. thesis.

Acknowledgement

Parameters and symbols of the methodology

Value	Symbol	Unit
Electric load	P	MW
Stochastic part of electric load	P^{stoch}	MW
Window size	s	min
Multifractal measure (parameter)	q	1
Multifractal fluctuation function	$F_q(s)$	MW
Generalized Hurst exponent	$H(q)$	1
Hurst exponent	$H \equiv H(2)$	1
Correlation Hurst exponent	$H^{cor}(q)$	1
Hurst exponent of shuffled time serie	$H^{shuf}(q)$	1
Scaling exponent	$\tau(q)$	1

References

[1] R. Weron, Modeling and Forecasting Electricity Loads and Prices: A Statistical Approach, John Wiley and Sons Ltd, 2006. 1, 2, 4

[2] J. Peirson, A. Henley, Electricity load and temperature: Issues in dynamic specification, Energy Economics 16 (4) (1994) 235 – 243. 1

[3] C.-C. Lee, Y.-B. Chiu, Electricity demand elasticities and temperature: Evidence from panel smooth transition regression with instrumental variable approach, Energy Economics 33 (5) (2011) 896 – 902. 1

[4] H. E. Hurst, Long term storage capacity of reservoirs, Trans. Am. Soc. Civ. Eng. 116 (770). 1, 2.2.2

[5] T. Preis, P. Virnau, W. Paul, J. J. Schneider, Accelerated fluctuation analysis by graphic cards and complex pattern formation in financial markets, New J. Phys. 11 (2009) 093024. 1

[6] R. Weron, A. Przybylowicz, Hurst analysis of electricity price dynamics, Physica A 283. 1, 2.1

[7] R. Weron, Energy price risk management, Physica A 285 (2000) 127. 1

[8] T.Preis, W. Paul, J. J. Schneider, Fluctuation patterns in high-frequency financial asset returns, Europhys. Lett. 82 (2008) 68005. 1

[9] B. B. Mandelbrot, J. W. Van Ness, Fractional brownian motions, fractional noises and applications, SIAM Review 10 (4) (1968) 422–437. 1

[10] H. A.Makse, S. Havlin, M. Schwartz, H. E. Stanley, Method for generating long-range correlations for large systems, Phys. Rev. E 53 (1996) 5445–5449. 1

[11] C.-K. Peng, S. V. Buldyrev, S. Havlin, M. Simons, H. E. Stanley, A. L. Goldberger, Mosaic organization of DNA nucleotides, Phys. Rev. E 49 (1994) 1685–1689. 1, 2.1, 2.2.2

[12] C.-K. Peng, S. V. Buldyrev, A. L. Goldberger, S. Havlin, F. Sciortino, M. Simons, H. E. Stanley, Long-range correlations in nucleotide sequence, Nature 356 (1992) 168–170. 1, 2.1, 2.2.2

[13] R. Mantegna, H. Stanley, An introduction to econophysics: correlations and complexity in finance, Cambridge University Press, New York, NY, USA, 2000. 1, 2.1

[14] C.-K. Peng, S. Havlin, H. E. Stanley, A. L.Goldberger, Quantification of scaling exponents and crossover phenomena in nonstationary heartbeat time series, Chaos 5 (1995) 82–87. 1, 2.1, 2.2.2, 2.3

[15] J. W. Kantelhardt, Y. Askenazy, P. C. Ivanov, A. Bunde, S. Havlin, T. Penzel, J.-H. Peter, H. E. Stanley, Characterization of sleep stages by correlations in the magnitude and sign of heartbeat increments, Phys. Rev. E 051908. 1, 2.1

[16] A. L. Goldberger, L. A. N. Amaral, L. Glass, J. M. Hausdorff, P. C. Ivanov, R. G. Mark, J. E. Mietus, G. B. Moody, C.-K. Peng, H. E. Stanley, PhysioToolkit, and PhysioNet: Components of a new research resource for complex physiologic signals, Circulation 101 (2000) e215–e220. 1, 2.3

[17] P. Talkner, R. O. Weber, Power spectrum and detrended fluctaution analysis: Application to daily temperatures, Phys. Rev. E 64 (2000) 150–160. 1, 2

[18] K. Koçak, Examination of persistence properties of wind speed records using detrended fluctuation analysis, Energy 34 (2009) 1980–1985. 1

[19] J. Kantelhardt, S. Zschiegner, E. Koscielny-Bunde, S. Havlin, A. Bunde, H. Stanley, Multifractal detrended fluctuation analysis of nonstationary time series, Physica A 316 (2002) 87. 1, 2.1, 2.2.2, 2.2.2

[20] J. Kantelhardt, E. Koscielny-Bunde, H. Rego, S. Havlin, A. Bunde, Detecting long-range correlations with detrended fluctuation analysis, Physica A 295 (2001) 441. 1, 2.1, 2.2.2, 2.2.2

[21] D. Horvatic, H. Staley, B. Podobnik, Detrended cross-correlation analysis for non-stationary time series with periodic trends, Europhys. Lett. 94 (18007). 1

[22] S. Chan, K. Tsui, H. Wu, Y. Hou, Y.-C. Wu, F. Wu, Load/price forecasting and managing demand response for smart grids: Methodologies and challenges, IEEE Signal Processing Magazine (2012) 68 – 85. 1

[23] T. Hong, P. Pinson, S. Fan, Global energy forecasting competition 2012, Int. J. Forecasting 30 (2) (2014) 357–363. 1

[24] R. Weron, Electricity price forecasting: A review of the state-of-the-art with a look into the future, Int. J. Forecasting 30 (2014) 1030–1081. 1

[25] A. Bunde, S. Havlin, J. W. Kanterhardt, T. Penzel, J. H. Peter, K. Voigt, Correlated and uncorrelated regions in heart-rate fluctuations during sleep, Phys. Rev. Lett. 85 (2000) 3736–3739. 2.1

[26] K. Hu, P. C. Ivanov, Z. Chen, P. Carpena, , H. E. Stanley, Effect of trends on detrended fluctuation analysis, Phys. Rev. E 64 (2001) 011114. 2.1, 2.2.2, 4

[27] S. Akselrod, D. Gordon, F. A.Ubel, D. C. Shannon, A. C.Barger, R. J.Cohen, Science 213 (1981) 220. 2.2.2

[28] C.-K. Peng, J. Mietus, J. M. Hausdorff, S. Havlin, H. E. Stanley, A. L. Goldberger, Long-range anticorrelations and non-gaussian behavior of the heartbeat, Phys. Rev. Lett 70 (9) (1993) 1343–1346. 2.2.2, 2.3

[29] H. Lavička, Simulations of Agents on Social Network, LAP Lambert Academic Publishing, 2010. 2.3

[30] H. P. Langtangen, A Primer on Scientific Programming with Python, Springer, 2009. 2.3

[31] I. Idris, NumPy 1.5 Beginner's Guid, Packt Publishing, 2011. 2.3

[32] K.-I. Sato, Lévy Processes and Infinitely Divisible Distributions, Cambridge University Press, 1999. 3.4.2

[33] J. Theiler, S. Eubank, A. Longtin, B. Galdrikian, J. Farmer, Testing for nonnonlinear in time series: the method of surrogate data, Physica D 58 (1992) 77–94. 3.4.2

[34] T. Schreiber, A. Schmitz, Surrogate time series, Physica D 142 (2000) 346–382. 3.4.2

[35] P. Norouzzadeh, W. Dullaert, B. Rahmani, Anti-correlation and multifractal features of spain electricity spot market, Physica A 380 (2007) 333–342. 3.4.2

[36] G. Samorodnitsky, M. S. Taqqu, Stable Non-Gaussian Random Processes: Stochastic Models with Infinite Variance., Chapman and Hall, New York, 1994. 3.4.2

[37] J. Nowicka-Zagrajek, R. Weron, Modeling electricity loads in California: ARMA models with hyperbolic noise, Signal Processing 82 (12) (2002) 1903 – 1915. 4

[38] S. S. Pappas, L. Ekonomou, D. C. Karamousantas, G. E. Chatzarakis, S. K. Katsikas, P. Liatsis, Electricity demand loads modeling using autoregressive moving average (ARMA) models, Energy 33 (9) (2008) 1353 – 1360. 4

[39] S. S. Pappas, L. Ekonomou, P. Karampelas, D. C. Karamousantas, S. K. Katsikas, G. E. Chatzarakis, P. D. Skafidas, Electricity demand load forecasting of the hellenic power system using an ARMA model, Electric Power Systems Research 80 (3) (2010) 256 – 264. 4

[40] Z. Boldiš, Czech electricity grid challenged by German wind, Europhys. News 44 (4) (2013) 16–18. doi:http://dx.doi.org/10.1051/epn/2013401. 4